Accepted Manuscript

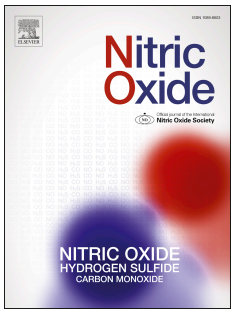

Zinc-induced root architectural changes of rhizotron-grown *B. napus* correlate with a differential nitro-oxidative response

Gábor Feigl, Árpád Molnár, Réka Szőllősi, Attila Ördög, Kitti Törőcsik, Dóra Oláh, Attila Bodor, Katalin Perei, Zsuzsanna Kolbert

PII: S1089-8603(19)30079-5

DOI: https://doi.org/10.1016/j.niox.2019.06.003

Reference: YNIOX 1906

To appear in: *Nitric Oxide*

Received Date: 6 March 2019

Revised Date: 27 June 2019

Accepted Date: 28 June 2019

Please cite this article as: Gá. Feigl, Áá. Molnár, Ré. Szőllősi, A. Ördög, K. Törőcsik, Dó. Oláh, A. Bodor, K. Perei, Z. Kolbert, Zinc-induced root architectural changes of rhizotron-grown *B. napus* correlate with a differential nitro-oxidative response, *Nitric Oxide* (2019), doi: https://doi.org/10.1016/j.niox.2019.06.003.

Zinc-induced root architectural changes of rhizotron-grown *B. napus* correlate with a differential nitro-oxidative response

Gábor Feigl[1*], Árpád Molnár[1], Réka Szőllősi[1], Attila Ördög[1], Kitti Törőcsik[1], Dóra Oláh[1], Attila Bodor[2,3], Katalin Perei[2,3], Zsuzsanna Kolbert[1]

[1]Department of Plant Biology, University of Szeged, H6726 Szeged, Közép fasor 52., Hungary

[2]Department of Biotechnology, University of Szeged, H6726 Szeged, Közép fasor 52., Hungary

[3]Institute of Environmental and Technological Sciences, University of Szeged, H6726 Szeged, Közép fasor 52., Hungary

Árpád Molnár: molnara@bio.u-szeged.hu

Réka Szőllősi: szoszo@bio.u-szeged.hu

Attila Ördög: aordog@bio.u-szeged.hu

Kitti Törőcsik: kittitorocsik@gmail.com

Dóra Oláh: olah.dora18@citromail.hu

Attila Bodor: bodor.attila@gmail.com

Katalin Perei: perei@bio.u-szeged.hu

Zsuzsanna Kolbert: kolzsu@bio.u-szeged.hu

[*]Corresponding author:

Gábor Feigl

e-mail: feigl@bio.u-szeged.hu

H6726 Szeged, Közép fasor 52. Hungary

Abstract

Roots have a noteworthy plasticity: due to different stress conditions their architecture can change to favour seedling vigour and yield stability. The development of the root system is regulated by a complex and diverse signalling network, which besides hormonal factors, includes reactive oxygen (ROS) - and nitrogen species (RNS). The delicate balance of the endogenous signal system can be affected by various environmental stimuli, such as the excess of essential heavy metals, like zinc (Zn). Zn at low concentration, is able to induce the morphological and physiological adaptation of the root system, but in excess it exerts toxic effects on plants.

In this study the effect of a low, growth-inducing, and a high, growth inhibiting Zn concentrations on the early development of *Brassica napus* (L.) root architecture and the underlying nitro-oxidative mechanisms were studied in a soil-filled rhizotron system.

The growth-inhibiting Zn treatment resulted in elevated protein tyrosine nitration due to the imbalance in ROS and RNS homeostasis, however its pattern was not changed compared to the control. This nitro-oxidative stress was accompanied by serious changes in the cell wall composition and decrease in the cell proliferation and viability, due to the high Zn uptake and disturbed microelement homeostasis in the root tips. During the positive root growth response, a tyrosine nitration-pattern reorganisation was observed; there were no substantial changes in ROS and RNS balance and the viability and proliferation of the root tips' meristematic zone decreased to a lesser extent, as a result of a lower Zn uptake.

The obtained results suggest that Zn in different amounts triggers different root growth responses accompanied by distinct changes in the pattern and strength of tyrosine nitration, proposing that nitrosative processes have an important role in the stress-induced root growth responses.

Highlights

- Different levels of Zn induce distinct alterations in the root growth of rapeseed
- Low Zn supplementation changes protein nitration pattern and stimulates root growth
- High Zn treatment increases nitrosative stress and nitration, inhibiting root growth
- Nitrosative processes have an important role in Zn-induced root growth responses

Keywords

Brassica napus, zinc, root growth, nitrosative stress, nitro-oxidative stress, protein tyrosine nitration

1. Introduction

Heavy metal (HM) contamination of soils and water is an actual and growing challenge for the environment and for agriculture as well. This has partly originated from anthropogenic activities such as mining, waste disposal or agricultural processes for instance the excessive use of fertilisers or application of sewage (Tóth et al. 2016), often causing higher Zn concentration than the typical 10-300 µg/g (ppm) in soils (Bacon and Dinev, 2005; Bi et al. 2006). Zinc (Zn) is the second most abundant metal in living organisms (Andreini and Bertini, 2009), possessing a fundamental role in diverse physiological processes. As the only metal represented in all six enzyme classes (Broadley et al. 2007), Zn is involved in carbohydrate, lipid and nucleic acid metabolism and protein synthesis as well. Even though it is indispensable, it can be phytotoxic in amounts greater than the optimal. Zn as a non-redox active element is able to tightly bind to oxygen, nitrogen or sulphur atoms, inactivating enzymes by binding to their cysteine residues (Nieboer and Richardson, 1980). Zn is able to promote secondary oxidative stress by the replacement of essential metal ions in catalytic sites (Schützendübel and Polle, 2002). During Zn-induced oxidative stress, several reactive oxygen species (ROS), like superoxide anion ($O_2^{\cdot-}$), hydrogen peroxide (H_2O_2), and hydroxyl radicals ($^{\cdot}OH$) are commonly generated (Morina et al. 2010; Jain et al. 2010; Gill et al. 2010). In order to ensure the plants' survival, the level of ROS has to be strictly regulated by a complex mechanism (Apel and Hirt, 2004), including numerous enzymatic antioxidants such as ascorbate peroxidase (APX; EC 1.11.1.11), glutathione reductase (GR; EC 1.6.4.2), catalase (CAT; EC 1.11.1.6) and superoxide dismutase (SOD; EC 1.1.5.1.1), or non-enzymatic antioxidants like ascorbate or glutathione.

In addition to ROS, reactive nitrogen species (RNS) are also being formed as the consequence of many different environmental stresses. The term RNS refer to the family of nitric oxide (NO) and associated molecules, including peroxynitrite ($ONOO^-$) and S-nitrosoglutathione (GSNO), (Wang et al. 2013). Nitrosative stress, analogue to oxidative stress is the consequence of the accumulation of the above-mentioned molecules in the plant cells, can be caused by numerous environmental factors (Corpas et al. 2007, 2011).

The metabolisms of ROS and RNS are connected at several points. The concept of nitro-oxidative stress has only recently become the subject of research in the field of plant biology (Corpas and Barrosso, 2013). A typical example of ROS-RNS crosstalk is the reaction of $O_2^{\cdot-}$ and NO resulting in the formation of $ONOO^-$, which is accountable for post-translational

modification protein tyrosine nitration, the covalent modification on specific tyrosines in proteins forming 3-nitrotyrosine (Corpas et al. 2013). The addition of the nitro group to one of the ortho carbons in the aromatic ring of tyrosine residues (Gow et al. 2004) results in steric and electronic perturbations, modifying the tyrosine's ability to keep the proper conformation of the proteins or to function in electron transfer reactions (van der Vliet et al. 1999). Tyrosine nitration might affect the function of the proteins in different ways: the most common outcome is the loss of the protein's function, but rarely gain of function or the lack of effect has also been reported (Greenacre and Ischiropoulos, 2001; Radi, 2004, Corpas et al. 2013). Moreover, tyrosine nitration is furthermore able to disturb signal transduction pathways by the inhibition of tyrosine phosphorylation (Galetsky et al. 2011).

Due to nitro-oxidative stress and disturbances in macro- and microelement homeostasis (Jain et al. 2010), excess Zn inhibits seed germination and plant growth (Mrozek and Funicelli, 1982; Wang et al. 2009) including root development (Lingua et al. 2008). HMs in high concentration lead to growth inhibition due to their phytotoxic effect by altering the most important plant physiological and metabolic processes (Kalaivanan and Ganeshamurthy, 2016), while on the other hand at low concentrations they are able to persuade the morphological and physiological adaptation of the root system called stress-induced morphogenic response (SIMR). SIMR is a special mixture of inhibition of primary root growth and induction of lateral root development, resulting in a shallower but horizontally more extensive root architecture, which most likely provides an enhanced stress tolerance (Potters et al. 2007; Kolbert 2016). A protection machinery in contradiction of enhanced HM concentrations is the modification of the cell wall in the root by the addition of e.g. callose or pectin. This process can assist the survival of the plant by restraining the uptake and translocation of HMs and by inhibiting the outflow of nutrients and assimilates (Sjölund, 1997; Chen and Kim, 2009), and at the same time cell wall alterations modify root growth processes as well.

Tracking the growth of the root system in soil can be challenging, however number of research apply rhizotrons to *in situ* observe root system architecture of e.g. maize (Jordan, 1992), trees (Pagés, 1992), *Arabidopsis* (Devienne-Barret et al. 2005) or *Brassica napus* under phosphorus deficiency (Yuan et al. 2016). Rhizotrons may vary in size, depending on the goal of the experiments and the investigated plant species, but in general their main feature is a transparent wall ensuring the *in situ* monitoring of the development of plants' root

system. In the present study, a 15 cm wide and 30 cm tall rhizotron system was developed, allowing the observation the early development of *Brassica napus* root system.

Contaminants, like Zn are able to change interactions between soil organisms (Krumins et al. 2015), hereby investigation of soil properties like enzyme activity can provide a more complete understanding of the effect of HM stress on plant-soil system (Hagmann et al. 2015). There are both examples of decreased (Wang et al. 2007) and increased (Kzlkaya, 2004; Pascual et al. 2004) enzyme functions due to contamination with different HMs, suggesting that soil microbial communities might be able to react differently to HM stress.

The crops' responses in their early developmental stage basically determine their subsequent development, thus studying of the zinc-induced changes in root architecture and the underlying mechanisms have a great significance. In a previous study we determined that *B. napus* is sensitive to Zn stress in a hydroponic system (Feigl et al. 2015), but no experiments were conducted in the topic in a near-natural (soil filled rhizotron) setup. Therefore, our goal was to compare growth-inducing and growth-inhibiting Zn concentrations in soil for *Brassica napus*, and to determine whether if the nitro-oxidative signalling network is involved in the development of these different growth responses.

2. Materials and methods

2.1. Rhizotron system

Custom-made plexi panels were assembled into 15 cm wide, 30 cm tall and 1.6 cm thick rhizotrons, using polifoam sheets and screws with wing nuts. The front panel is made of 3 mm thick, anti-glare, 100% transparent plastic, while the back panel is a 3 mm thick non-transparent black sheet; the thickness of the soil layer inside the rhizotron was 1 cm (Fig. 1). The rhizotrons were filled with Klasmann Potgrond P blocking substrate (100% frozen through black peat with a fine structure of maximum 8 mm size, pH 6.0; 210 mg N/l; 240 mg P_2O_5/l, 270 mg/l K_2O, 60.21 mg/kg (ppm) Zn) mixed with 20% sand; the initial water content was set to 70%. Based on preliminary experiments, 10 and 500 ppm Zn supplementation were chosen as acclimation-causing (growth-inducing) and growth-inhibiting concentrations, respectively; Zn supplementation was homogeneously distributed in the mixture by manual mixing.

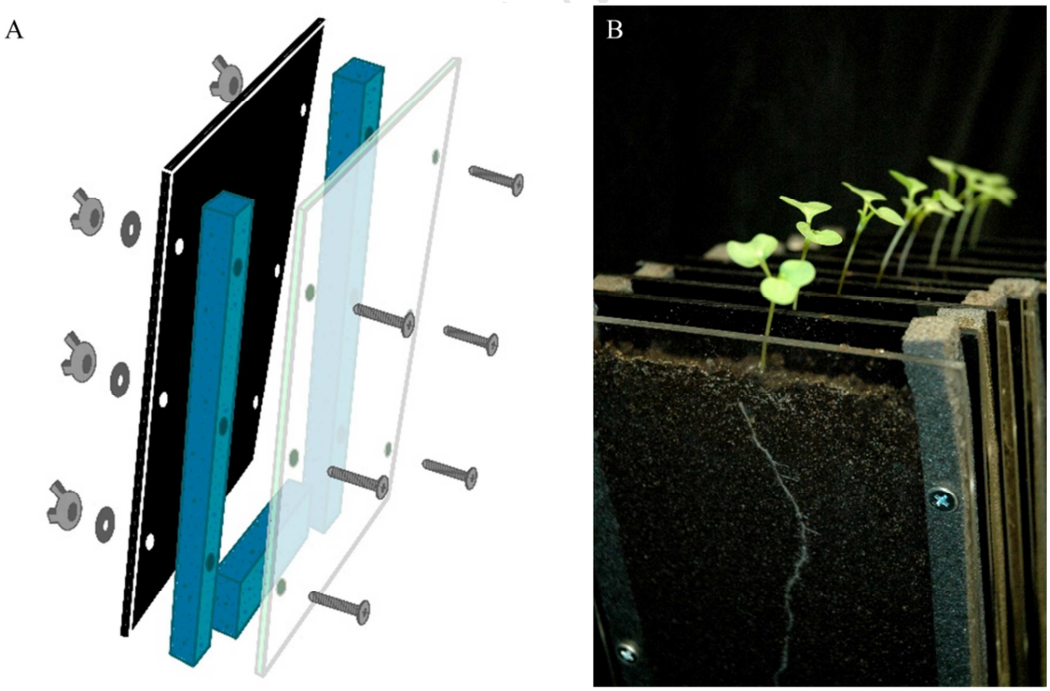

Fig. 1. Rhizotron design (A) and growing *Brassica napus* seedlings in soil-filled rhizotrons (B)

2.2. Plant material and growing conditions

Brassica napus L. (GK Gabriella; oilseed rape or rapeseed) seeds provided by the Cereal Research Non-Profit Ltd. (Szeged, Hungary) were pre-germinated for 24 hours at 26°C and germinated seeds were transferred to the soil surface of the pre-filled rhizotrons (one seed per rhizotron, Fig 1B). During the first 48 hours after the sowing, the seedlings were covered with transparent plastic foil to provide optimal humidity, then the growing plants were supplemented with 10 ml distilled water on every second day. Seedlings were cultivated in greenhouse at photon flux density of 150 µmol m^{-2} s^{-1} (12/12h light/dark cycle) at a relative humidity of 55-60% and 25±2°C for 10 days, then the rhizotrons were scanned, disassembled and the roots were cleaned for further examination. In some cases, daily scanning was also performed to obtain images for the representation of the growth dynamics of the root system (Supplementary video 1).

2.3. Morphological measurements

Scanned images of the rhizotrons were analysed using Fiji software (http://fiji.sc/Fiji; Schindelin et al. 2012). The length of the primary root (PR; mm) was measured; the number of visible lateral roots were counted (LR; laterals per root) and their length (mm) and angle included with the vertical direction (degrees) were also measured. These data were acquired from eight to ten separate generations, in each generation eight plants were examined (n=8).

2.4. Element content analysis

The concentrations of microelements were measured by inductively-coupled plasma mass spectrometry (ICP-MS, Thermo Scientific XSeries II, Asheville, USA) according to Lehotai et al. (2012). Values of Zn and other microelement concentrations (Fe, Cu, Mn, Ni, Cr, Co and Mo) are given in µg/g dry weight (DW). Bioaccumulation factor (BAF, Zn concentration in the shoot/Zn concentration in the soil) and translocation factor (TF, Zn concentration in the shoot/Zn concentration in the root) was calculated according to Rezvani and Zaefarian (2011). This analysis was carried out twice with three samples each (n=3).

2.5. Microscopic determination of Zn distribution, callose and pectin deposition, lipid peroxidation, viability and DNA replication capability in the root tissues

For the detection of Zn uptake, root tips were washed in PBS buffer (137 mM NaCl, 2.68 mM KCl, 8.1 mM Na_2HPO_4, 1.47 mM KH_2PO_4, pH 7.4), and then dyed with 25 µM Zinquin (ethyl (2-methyl-8-p-toluenesulphonamido-6-quinolyloxy)acetate) in PBS for 1 h at room temperature in darkness as described by Sarret et al. (2006).

Callose content of the root tips' cell walls was visualised by using aniline blue staining according to Feigl et al. (2015). Roots tips were dyed in aniline blue solution (0.1%, w/v in 1M glycine) for 5 min, then replaced by distilled water prior to microscopic analysis.

Cell wall pectin content was detected by using 0.05% (w/v) ruthenium red (RR) solution prepared with distilled water, according to Durand et al. (2009).

Viability of meristematic cells in the root was determined by fluorescein diacetate (FDA) staining, according to Lehotai et al. (2011); roots were dyed with 10 µM staining solution prepared in 10 mM MES (4-morpholineethanesulfonic acid) / 50 mM KCl buffer (pH 6.15). FDA is a cell membrane-permeant esterase-substrate, which is widely used as a viability probe, which measures enzymatic (intracellular esterase) activity (it is required to activate its fluorescence) and membrane integrity (it is required for the retention of the fluorescent product) (McCabe and Leaver, 2000).

To evaluate DNA replication prior to cell proliferation in root tips 5-ethynyl-2′-deoxyuridine (EdU) was used as described by Nakayama et al. 2015 with slight modifications. Root segments were incubated in 20 µM EdU solution (prepared in PBS) in darkness for 2 hours followed by incubation in detergent buffer (PBS buffer pH 7.4 containing 4% formaldehyde and 0,5% Triton X-100). Samples were washed tree times with PBS and incubated for 30 minutes in reaction buffer (40 mM ascorbate, 4.2 mM $CuSO_4$ and 3.6 µM Alexa Fluor 488 azide in PBS). To determine the number of cells in which EdU incorporation has occurred in the apical meristem, fluorescent cells were counted within circles of 50 µm radii. These measurements were carried out twice with 10-15 samples each (n=10-15).

2.6. Detection of ROS and RNS

Fluorescence consistent with superoxide anion in the root tips was detected by using dihydroethidium (DHE) (30 min incubation in darkness at 37°C with 10 µM dye solution followed by two washing with 10 mM Tris/HCl, pH 7.4) (Pető et al. 2013). Fluorescence consistent with hydrogen peroxide was detected by the incubation of root tips in 50 µM

Ampliflu™ (10-acetyl-3,7-dihydroxyphenoxazine, ADHP or Amplex Red) solution (prepared in 50 mM sodium-phosphate buffer, pH 7.5), according to Lehotai et al. (2012).

Fluorescence consistent with NO in *Brassica* root tips were determined by 4-amino-5-methylamino-2',7'-difluorofluorescein diacetate (DAF-FM DA), by incubation in 10 µM dye solution prepared in 10 mM Tris/HCl buffer, (pH 7.4) for 30 min in darkness at room temperature (Kolbert et al. 2012). Fluorescence consistent with peroxynitrite was visualised with 10 µM dihydrorhodamine 123 (DHR) prepared in Tris-HCl buffer. After 30 min of incubation, root tips were washed with buffer two times (Sarkar et al. 2014).

These measurements were carried out twice with 10-15 samples each (n=10-15). Suppl. fig. 5 shows positive and negative controls for the applied fluorescent dies.

2.7. Immunofluorescent microscopic detection of 3-nitrotyrosine in root tissues

For immunofluorescent staining, small pieces of root samples derived from the root tips were fixed in 4% (w/v) paraformaldehyde according to Barroso et al. (2006). Following fixation, root samples were rinsed with distilled water and fixed in 5% agar (bacterial; Zelko et al. 2012 with modifications). Then 100 µm thick longitudinal sections were made using a vibratome (VT 1000S, Leica).

Immunodetection of 3-nitrotyrosine was carried out according to Valderrama et al. (2007) as described by Kolbert et al. (2018).

Immunofluorescent detections were carried out on two separate plant generations with 8 plants examined in each (n=8).

2.8. Acquisition and processing of microscopic images

Brassica root samples labelled with different fluorescent dyes were examined under a Zeiss Axiovert 200M inverted microscope (Carl Zeiss, Jena, Germany). Filter set 9 (exc.: 450-490 nm, em.: 515- ∞ nm) was used for DHE; filter set 10 (exc.: 450-490, em.: 515-565 nm) was applied for DAF-FM, DHR, FDA and FITC; filter set 20HE (exc.: 546/12, em.: 607/80) was used in case of AmplexRed and filter set 49 (exc.: 365 nm, em.: 445/50 nm) was utilised with aniline blue, EdU and Zinquin staining.

Fluorescence intensities (pixel intensity, consistent with the amount of the detected molecule) in the meristematic zone were measured on the acquired images using Axiovision Rel. 4.8 software within circles of 50 µm radii.

2.9. Determination of soil catalase activity

Activity of catalase in soil was measured by a titrimetric method according to Stępniewska et al. (2009). 2 g soil from each rhizotron was added to a mixture of 40 mL distilled water and 5 mL 0.3% H_2O_2. After 20 minutes of shaking, 5 mL of 1.5 M H_2SO_4 was added and the suspension was filtered, then titrated with 0.02 M $KMnO_4$. Catalase activity (CAT) was expressed as µmol H_2O_2/g dry soil weight/min calculated from the reacted amount of 0.02 M $KMnO_4$. Soil samples without H_2O_2 addition were used as blanks.

This measurement was carried out on two separate generations with 3 examined soil sample each (n=3).

2.10. Measurement of root SOD activity and SOD isoform staining on native-PAGE

SOD (EC 1.15.1.1) activity of *Brassica napus* roots was determined according to (Dhindsa et al. 1981), as described by Feigl et al. (2015); enzyme activity is expressed in Unit/g fresh weight. SOD isoforms were detected in gels by the modified method of Beauchamp and Fridovich (1971) as described by Feigl et al. (2015).

These experiments were carried out on two separate plant generations with three samples examined each (n = 3).

2.11. NADPH-oxidase (NOX) activity of the roots on native-PAGE

NOX activity was examined on 10% native polyacrylamide gels by the NBT reduction method of Gémes et al. (2016) with slight modifications published by Kolbert et al. (2018). 25 µl of protein extracts were loaded in each well.

These experiments were carried out on two separate plant generations with three samples examined each (n = 3).

2.12. GSNOR activity on native-PAGE

GSNOR activity was visualized using a slightly modified method of Seymour and Lazarus (1989) and is described in detail by Kolbert et al. (2018). 50 µl of protein extracts were loaded in each well.

These experiments were carried out on two separate plant generations with three samples examined each (n = 3).

2.13. SDS-PAGE and western blotting for NO-Tyr and GSNOR

Protein extracts of *Brassica napus* root tissues were prepared as described in Kolbert et al. (2018); protein concentration was determined using the Bradford (1976) assay with bovine serum albumin as a standard. 20 µl of root protein extracts per lane were subjected to sodium dodecyl sulphate-PAGE (SDS-PAGE) on 12% acrylamide gels, followed by procedures described by Kolbert et al. (2018).

Immunoassay for GSNOR enzyme was performed using a polyclonal primary antibody from rabbit diluted 1:2000 purchased from Agrisera (AS09 647). As secondary antibody affinity-isolated goat anti-rabbit IgG–alkaline phosphatase secondary antibody (Sigma-Aldrich, cat. No. A3687) was used at a dilution of 1:10000, and bands were visualized by using the NBT/BCIP (nitroblue tetrazolium/5-bromo-4-chloro-3-indolyl phosphate) reaction.

Western blot was applied to three separate protein extracts from different plant generations, multiple times per extract, giving a total of six blotted membranes (n = 3).

Protein bands of SOD, NOX, GSNOR enzyme and nitrated proteins were quantified by Gelquant software provided by biochemlabsolutions.com.

2.14. Statistical analysis

The results are expressed as the mean ± s.e. Multiple comparison analyses were performed with SigmaStat 12 software using analysis of variance (ANOVA; $P<0.05$) and Duncan's test. In some cases, Microsoft Excel 2010 and Student's t-test were used (*$P\leq0.05$, **$P\leq0.01$, ***$P\leq0.001$).

3. Results and discussion

3.1. Zn uptake-induced changes in root architecture, root cell wall composition and microelement homeostasis

As previously stated, control soil contained 60 ppm total Zn, thus 10 and 500 ppm Zn supplementation resulted in 70 (within the typical 10-300 ppm range) and 560 ppm (over the typical range) total soil Zn content, respectively. Zn exists in five distinct pools in soils such as water soluble, exchangeable, adsorbed, chelated or complexes of Zn (Noulas et al. 2018, however the investigation of the form and bioavailability of the total Zn in the soil were not our aim, thus were not examined. Throughout the article control refers to soil containing 60 ppm Zn, as provided by the manufacturer.

The rhizotron system allows the easy monitoring of the development of the root system architecture (RSA) (Fig 2A). Compared to the control, both Zn supplementations caused significant changes in the RSA (for the dynamics of RSA development see supplementary video 1). Mild Zn treatment (10 ppm supplementation) induced root growth in terms of the length of the primary root (107%) and number of lateral roots (129%) (Fig 2B, C), while the length of lateral roots remained similar to the control (Fig 2D). On the other hand, high Zn concentration (500 ppm supplementation) inhibited primary and lateral root elongation (58 and 48%, respectively) (Fig 2B, D), while the number of lateral roots (similar to the 10 ppm supplementation) were higher than in the control (125%) (Fig 2 C). It can be noted, that due to the significant shortening of the primary root under 500 ppm Zn supplementation, lateral root density increased noticeably compared to control conditions (LR/cm; control: 0.5, 500 ppm Zn: 1.1). In a previous, hydroponic study, lateral root number of *B. juncea* and *B. napus* was also increased by Zn excess (Feigl et al. 2016); and this phenomenon is also a known symptom of SIMR (Potters et al. 2009). Moreover, in *Sesbania* species, Zn also induced lateral root formation (Yang et al. 2004). Interestingly, the angle of lateral roots relative to the vertical direction also changed significantly due to Zn supplementation, but the response was different depending on Zn concentrations: addition of 10 ppm Zn induced a more horizontal lateral root growth (control: 65°, 10 ppm Zn 68°), while 500 ppm Zn supplementation led to a more vertical (60°) lateral root orientation (Suppl. fig. 1). This contrasting response corroborate the opposite effect of the two applied Zn treatment: low Zn-induced growth induction is accompanied by a more horizontal root system (acclimation), while the growth-inhibiting Zn concentration caused the lateral roots to grow more to the vertical direction,

possibly as compensational reaction. According to our hypothesis, since the PR growth is inhibited by 500 ppm Zn supplementation, the LRs are aiming to the deeper zones, while addition of 10 ppm Zn did not inhibit PR growth and the LRs are expanding laterally, since they are able acclimatise to the mild Zn treatment. Many studies discuss the regulation of root angle determination by a complex series of internal and external factors (Toal et al. 2018), however the existence or background of Zn-induced changes in the lateral root angle is yet to be discovered.

According to the obtained RSA data, the two applied Zn concentrations causes two distinctly different responses: the effect of 10 ppm Zn supplementation has an overall positive consequence, while 500 ppm Zn supplementation inhibits longitudinal growth (PR and LR) and induces branching process at the same time. It has to be also noted that though 500 ppm Zn treatment caused responses that could even meet the requirements of SIMR (Potters et al. 2009), however its negative, growth inhibiting effects are more pronounced.

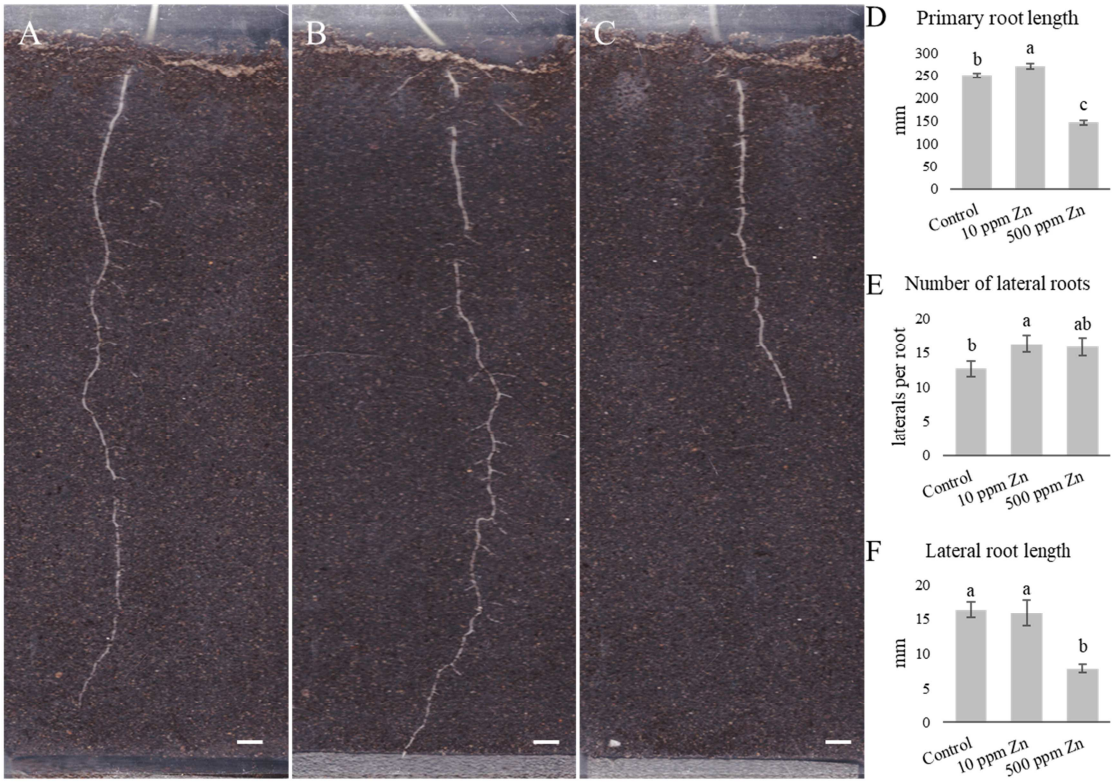

Fig. 2. (ABC) Representative images of the effect of Zn on the root system architecture of 10-days-old *B. napus*. (A – control, B – 10 ppm Zn supplementation, C – 500 ppm Zn supplementation; bar=1cm). Length of the primary root (D) and the effect of Zn on the number (E) and length (F) of lateral roots. Different letters indicate significant differences according to Duncan-test (n=8, $P<0.05$).

Microscopic analysis of the Zn content in the root apical meristem (RAM) revealed that the meristematic zones of plants grown in the 10 ppm Zn supplemented soil did not accumulate significantly more Zn than the control, while the addition of 500 ppm Zn caused significant Zn uptake (3.5-fold increase) in their root apical meristems (Fig 3A). Root cell wall modifications can indicate and prevent heavy metal uptake. Callose content of the root tips shows a similar tendency to the Zn contents, namely only the high Zn concentration caused significant (almost two-fold, compared to the control) callose deposition (Fig 3B). Excess Zn reportedly caused significant callose deposition in e.g. bean (Peterson and Rauser, 1979) and *B. juncea* and *B. napus* (Feigl et al. 2015). The high amount of deposited callose might contribute to growth inhibition, since it decreases cell wall loosening and inhibits symplastic transport (Jones et al. 2006; Piršelová et al. 2012). Callose is not permeable to metal ions (Hall, 2002), thus prevents Zn to enter the cells. On the other hand, both Zn treatments increased pectin content in the root tips, providing a possible explanation how 10 ppm Zn-treated root meristem is able to exclude Zn. Although, in case of 500 ppm Zn addition, RAM showed more pronounced pectin staining compared to 10 ppm Zn treatment (Fig 3C). Pectin is able to bind HMs in the cell walls (Krzesłowska, 2011) and the observed pectin accumulation due to the 10 ppm Zn treatment could be enough to exclude Zn but probably it was not sufficient against 500 ppm Zn supplementation. The observed changes in pectin and callose content could complement each other: the increase of pectin may bind Zn in the cell wall, and the deposited callose immobilizes it in the cell wall and ensures that it does not enter the cytoplasm. The latter can contribute to the above discussed growth inhibition as well.

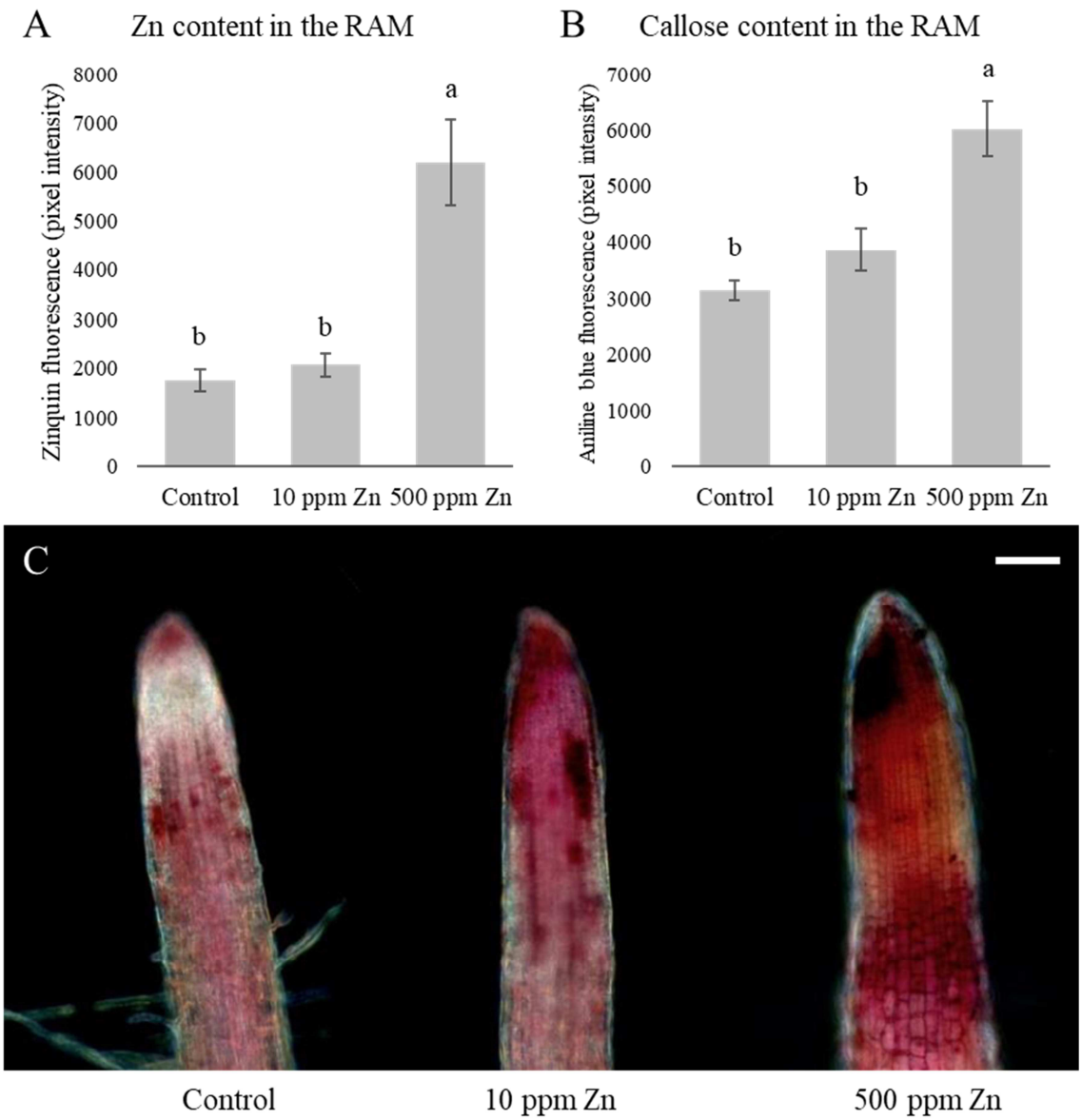

Fig. 3. Zinc (A) and callose (B) content in the root apical meristem of 10 days-old *Brassica napus* grown in soil-filled rhizotrons in the presence of optimal (control, 60 ppm Zn) or supraoptimal (10 and 500 ppm supplementation) Zn levels. Different letters indicate significant differences according to Duncan-test (n=10-15, P<0.05). (C) Representative image showing the pectin-associated pink colorization in the *Brassica napus* root tips (bar=100µm).

According to the ICP-MS measurements Zn content of the whole root system was significantly increased by both Zn treatments in a concentration dependent manner (2.8 and 175-fold, compared to the control) (Table 1). Additionally, Zn was translocated to the shoot in a concentration-dependent manner. Bioaccumulation factor (BAF, shoot/soil concentration ratio) is a suitable tool to assess the plants' metal accumulation potential hence their phytoremediation ability (Zhao et al. 2003). The BAF under control circumstances was 3.19, while 10 and 500 ppm Zn treatment enhanced it to 5.32 and 4.77, respectively, proving that *B.*

napus is a moderate Zn accumulator species, since in excluder plants this value is below 1 (Ebbs and Kochian 1997). Also, in our previous works, similar Zn accumulation tendencies were observed (Feigl et al. 2015, 2016). Translocation factor (TF), as Zn concentration ratio of plant shoots to roots can also be used to evaluate a species' phytoremediation potential (Yoon et al. 2006). Contrary to BAF values, TF proportionally decreased by the increasing external Zn concentration (0.74; 0.51 and 0.05, respectively), indicating that though rapeseed is a moderate accumulator, it's translocation capacity is low.

Zn supplementation of the soil also modified the microelement homeostasis of Brassica roots. Iron (Fe), cobalt (Co) and molybdenum (Mo) content of the roots decreased in a concentration-dependent manner, while the decline of copper (Cu), nickel (Ni), chromium (Cr) concentrations was not proportional to the increasing Zn concentration (Table 1). On the other hand, manganese (Mn) content increased due to the Zn supplementation in a concentration-dependent way (Table 1). There is evidence published about the crosstalk of Zn and another elements like Fe, Cu and Cd, but a comprehensive evaluation is still lacking (Jain et al. 2013). In *Arabidopsis thaliana* roots, Zn treatment caused decreased Fe and Cu content (Jain et al. 2013), while in *A. halleri* Zn treatment reduced Ni (Zhao et al. 2001) and Mn (Küpper et al. 2000) content of the roots. In the present experimental system, excess Zn decreased the *in planta* concentrations of relevant microelements like Fe, Cu, Mo, Co, Cr thus disturbing microelement homeostasis of *B. napus* roots which in turn may contribute to growth reduction.

A	Control	10 ppm Zn	500 ppm Zn
Zn root (µg/g DW)	258.7 ± 3.87 [c]	723.3 ± 22.15 [b]	45300 ± 109.6 [a]
Zn shoot (µg/g DW)	191.8 ± 0.84 [c]	373 ± 2.98 [b]	2672 ± 32.57 [a]
BAF Zn	3.19	5.32	4.77
TF Zn	0.74	0.51	0.05

B	Control	10 ppm Zn	500 ppm Zn
Fe root (µg/g DW)	744.9 ± 4.81 [a]	515 ± 4.02 [b]	284.9 ± 2.48 [c]
Cu root (µg/g DW)	56.01 ± 0.95 [a]	9.06 ± 0.44 [b]	9.32 ± 0.05 [b]
Mn root (µg/g DW)	233.5 ± 1.73 [c]	240.8 ± 2.06 [b]	322.9 ± 1.25 [a]
Ni root (µg/g DW)	267.3 ± 1.33 [a]	3.93 ± 0.19 [b]	3.40 ± 0.13 [b]

Cr root (µg/g DW)	23.37 ± 0.36 [a]	0.53 ± 0.04 [b]	0.74 ± 0.02 [b]
Co root (µg/g DW)	3.04 ± 0.09 [a]	2.38 ± 0.03 [b]	0.86 ± 0.01 [c]
Mo root (µg/g DW)	0.94 ± 0.05 [a]	0.85 ± 0.02 [b]	0.46 ± 0.02 [c]

Table 1. (A) Zn content of the *B. napus* organs and BAF/TF values. (B) Microelement content of the roots (µg/g DW). Different letters indicate significant differences according to Duncan-test (n=3, $P<0.05$).

3.2. Distinct tyrosine nitration response associated with different root architectural changes

Protein tyrosine nitration, a posttranslational modification is observed to participate in many physiological and stress-related processes (Kolbert et al. 2017) and proved to be a suitable biomarker in case of Zn-stressed *Brassica* species in hydroponics (Feigl et al. 2015, 2016). The presence of tyrosine nitration has been proved in control, healthy plants as well (Corpas et al. 2013; Feigl et al. 2015; Lehotai et al. 2016). In the present experimental setup six nitrated protein bands were detectable in the 35-10 kDa molecular weight zone (Fig 4A) under control circumstances, proving that a physiological nitroproteome is present in soil-grown roots as well. The low and high Zn concentrations caused a diverse response. 10 ppm Zn supplementation caused a tyrosine nitration-pattern rearrangement: the nitration of several protein bands decreased that were nitrated under control conditions, while four newly nitrated protein bands appeared (approximately 250, 50, 45 and 23 kDa) (Fig 4A, white arrows). In contrast, 500 ppm Zn treatment resulted in a generally increased tyrosine nitration in the lower molecule weight zone (Fig 4A, same bands as in control roots, black arrows), and also a newly nitrated protein band appeared (approximately 25 kDa) (Fig 4A). The existence of a basal nitration state of the protein pool is observed in many species (reviewed in Kolbert et al. 2017), and previous studies also found that Zn induces increased tyrosine nitration in the roots of *B. napus* (Feigl et al. 2015, 2016). The pattern and rate of tyrosine nitration however is different in the present study compared to the previous results, possibly because of the different experimental setup (hydroponics vs soil filled rhizotron) and applied Zn concentrations.

We also detected protein tyrosine nitration *in situ* in the root tips, and the overall strength of the tyrosine nitration-dependent fluorescence showed correlation with the previous results: compared to the control, fluorescence did not increase significantly in the 10 ppm Zn-treated

root tips, while it was considerably higher in the 500 ppm Zn-treated roots. Protein tyrosine nitration is a result of a series of changes in the nitro-oxidative signalling network, and the responsible carbonate, hydroxyl radicals and nitrogen dioxide radicals are derived from peroxynitrite ($ONOO^-$) (reviewed in Kolbert et al. 2017). The Zn-triggered changes in fluorescence consistent with $ONOO^-$ formation show similar tendencies like the level of tyrosine nitration, since compared to the control, only the 500 ppm Zn treatment induced significant $ONOO^-$-associated fluorescence increment (Fig 4C), also corroborating tyrosine nitration results.

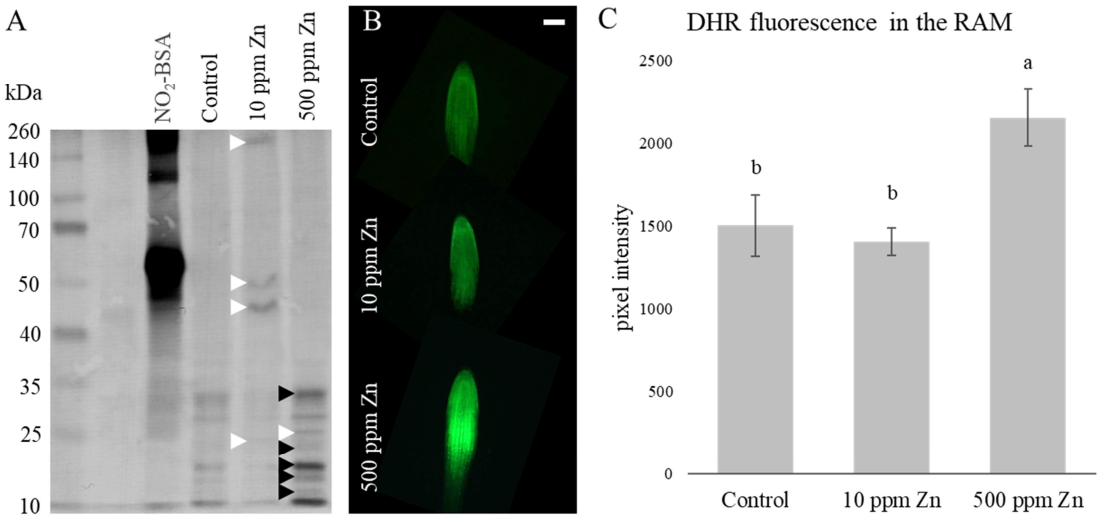

Fig. 4. Representative immunoblot showing protein tyrosine nitration in the roots of *B. napus* grown in soil-filled rhizotrons under control circumstances (60 ppm Zn) and Zn supplementation (A). White arrows show newly nitrated protein bands while black arrows show protein bands with increased nitration compared to the control (n=3). (B) Immunolocalisation of 3-nitrotyrosine in root tips of *B. napus* grown in soil-filled rhizotrons under control circumstances and Zn supplementation (bar=100µm). (C) Changes in the fluorescence consistent with peroxynitrite in the root apical meristem of *B. napus* upon Zn treatment. Different letters indicate significant differences according to Duncan-test (n=10-15, $P<0.05$).

3.3. Distinctive changes in the underlying nitro-oxidative signal transduction network

Peroxynitrite is derived from superoxide anion and nitric oxide, thus the amount of $ONOO^-$ and ultimately the appearance of tyrosine nitration depends on the production and accumulation of these reactive species (Kolbert et al. 2017). Similar to $ONOO^-$, fluorescence consistent with NO formation in the root apical meristem was increased only by 500 ppm Zn

treatment (Fig 5A). NO can be also stored in the form of S-nitrosoglutathione (GSNO), which can act as a mobile NO reservoir (Begara-Morales et al. 2018). GSNO can either spontaneously decompose to NO or can be enzymatically reduced by GSNOR to GSSG and NH_3 (Lindermayr 2018). Zn treatment, especially 500 ppm Zn supplementation, increased both GSNOR enzyme activity (Fig 5C and suppl. fig. 2) and protein amount (Fig 5D), however the reason behind the size-shift of the immunopositive band is yet unknown. The higher NO-associated fluorescence discussed above can be related to the higher activity and presence of GSNOR, which is responsible for GSNO removal, suggesting that Zn induces a severe disturbance in NO homeostasis in the roots treated with 500 ppm Zn.

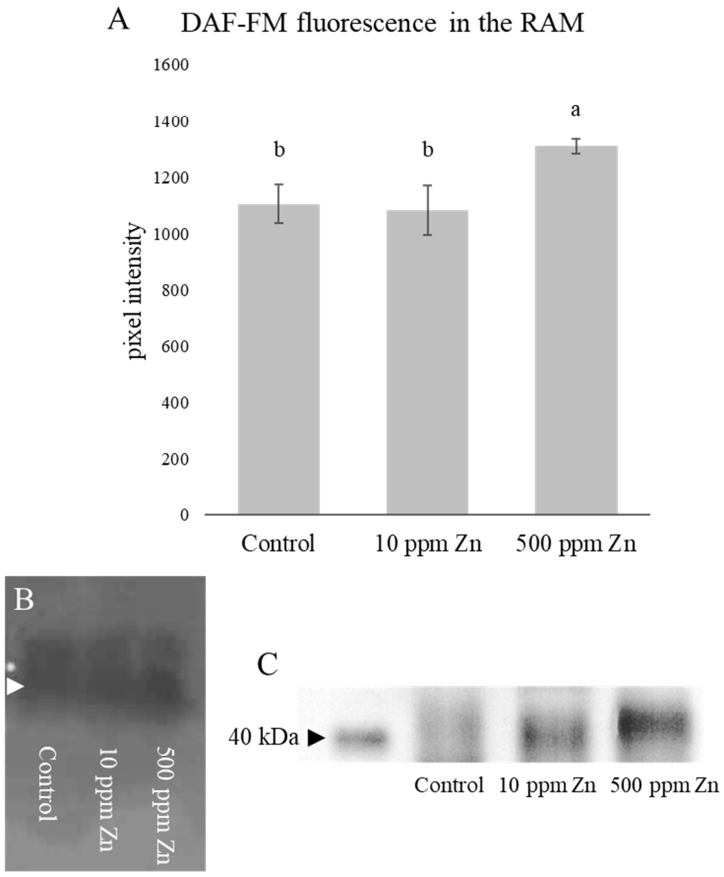

Fig. 5. Fluorescence consistent with NO formation in the root apical meristem of *B. napus* grown in soil-filled rhizotrons containing optimal (control, 60 ppm total Zn) or supraoptimal (10 ppm and 500 ppm Zn supplementation) Zn concentrations. (A). Different letters indicate significant differences according to Duncan-test (n=10-15, $P<0.05$). Representative native-PAGE (6%) of *B. napus* root extracts and staining for GSNOR activity (white arrow) (B). Representative immunoblot showing GSNOR protein abundance in roots of control or Zn-treated *B. napus* (C) (n=3).

Besides the homeostasis of reactive nitrogen species, the balance of reactive oxygen species was also changed by Zn treatment. Both Zn treatment increased the fluorescence consistent with superoxide formation in the root tips, regardless of the applied concentration (Fig 6B). The native-PAGE analysis of the $O_2^{\cdot-}$ producing NADPH oxidase enzyme revealed five isoenzymes, and the total activity of this enzyme decreased in a concentration-dependent way (Fig 6A, for separate izoenzyme activities see suppl. fig. 3), suggesting that there is an another source of $O_2^{\cdot-}$ in the root tips, like plant peroxidases that mainly generate $O_2^{\cdot-}$ through oxidation of phenolic compounds (Kimura et al. 2014). Measurement of the SOD activity shown increment only in case of 500 ppm Zn treatment (Fig 6C), and the native-PAGE analysis of the enzyme identified that there is a rearrangement of isoenzyme activities (Fig 6D). While the overall SOD activity in case of 10 ppm Zn treatment did not change significantly, in the background a very slight increment in the Mn and Fe-SOD isoenzyme-activity could be detected (Suppl. fig. 4AB). On the other hand, in case of 500 ppm Zn treatment, Fe-SOD isoenzyme activity decreased notably, while the activity of all three Cu/Zn-SOD isoenzymes increased significantly (Suppl. fig. 4C). One of the reason of the decreased Fe-SOD activity could be the reduced availability of iron as previously shown in Table 1, while the also reduced accessibility of copper did not affect Cu/Zn-SOD activity in a negative way.

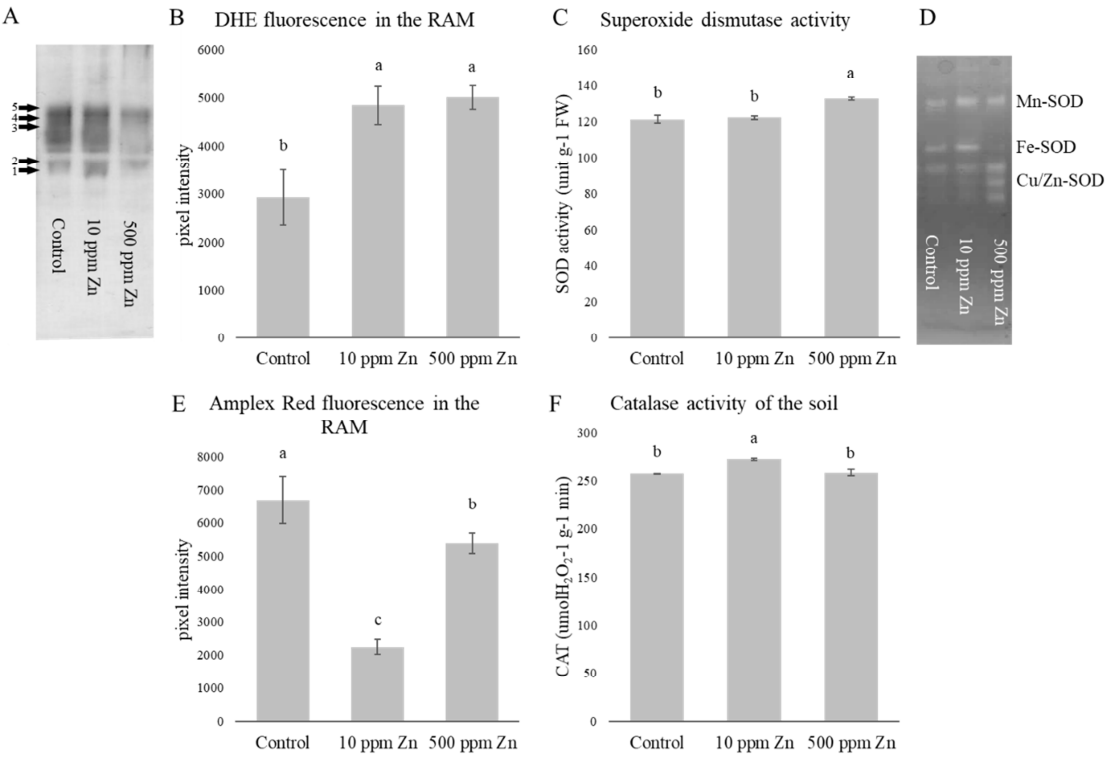

Fig. 6. (A) Native-PAGE (10%) separation of NADPH oxidase isoenzymes in the root of *B. napus* supplemented with 10 and 500 ppm Zn, compared to the control (60 ppm total Zn). Putative isoenzymes are numbered and indicated by black arrows. (B) Fluorescence consistent with superoxide formation in the root apical meristem. Total superoxide dismutase activity (C) and superoxide dismutase isoenzymes separated on native-PAGE (10%) (D). (E) Fluorescence consistent with H_2O_2 formation in the root apical meristem of *B. napus* and (F) catalase activity of the soil supplemented with 10 and 500 ppm Zn. Different letters indicate significant differences according to Duncan-test (n=3 (SOD, CAT) or 10-15 ($O_2^{\cdot -}$ and H_2O_2), $P<0.05$).

Fluorescence consistent with hydrogen peroxide formation in the root tips decreased significantly after Zn treatment, and the different amounts of supplied Zn caused different responses. The H_2O_2-associated fluorescence of the root tips was the lowest in case of 10 ppm Zn supplementation (Fig 6E); however, the activity of SOD in the roots did not explain this difference. Therefore, as an interesting possibility, soil CAT activity was examined. As the effect of Zn supply, the CAT activity in the soil increased significantly in case of 10 ppm Zn supplementation (Fig 6F), which was accompanied by the lowest H_2O_2-related fluorescence in the root tips, suggesting that somehow the growth medium may be able to buffer/extinguish the produced H_2O_2 in the root apical meristem. The CAT activity in the soil partly depends on the total number of aerobic heterotrophic bacteria (measured with colony forming unit counting), which was only negatively affected by the 500 ppm Zn treatment, while the addition of 10 ppm Zn slightly increased bacterial counts in the growth media (data not shown). Also, micromycetes, as the members of soil microbial communities often produce extracellular catalases (Kurakov et al. 2001), providing a further explanation for decreased fluorescence consistent with H_2O_2 formation in the root tips. In general, heavy metal contamination can either lower (Kandeler et al. 2000) or increase (Kzlkaya, 2004; Pascual et al. 2004) the enzymatic activities of soil microbial communities, showing the complexity of the heavy metal induced responses of soil enzyme activities. Belyaeva et al. (2005) reported that catalase is inhibited by Zn stress, although this inhibition is much less pronounced than invertase or urease activity loss.

3.4. Subsequent viability loss of the root tips

Viability of the root apical meristem seriously affects the growth of the root system. The above discussed Zn uptake and Zn-induced changes in the nitro-oxidative homeostasis affects the development of the root system by modifying the viability and proliferation rate of the apical meristem. According to the fluorescent EdU staining, which detects cell DNA synthesis

(Salic and Mitchison, 2008), the number of cells with active DNA replication decreased significantly by both Zn treatment (by 33 and 77%, respectively) (Fig 7AB).With FDA staining we detected the viability of the root apical meristem, and it showed similar changes as seen in the number of proliferating cells, both Zn supplementations caused significant decrease in their viability (by 45 and 75%, respectively, compared to the control, if that's fluorescence is defined by 100%) (Fig. 7C), suggesting that the cells with decreased DNA replication activity correlate closely with the viability of the meristematic cells. These results do not necessarily coincide with the primary root growth data, since besides proliferation and viability, many other factors (alterations in the primary metabolism or changes in the hormonal homeostasis) influence primary root elongation (Satbhai et al. 2015).

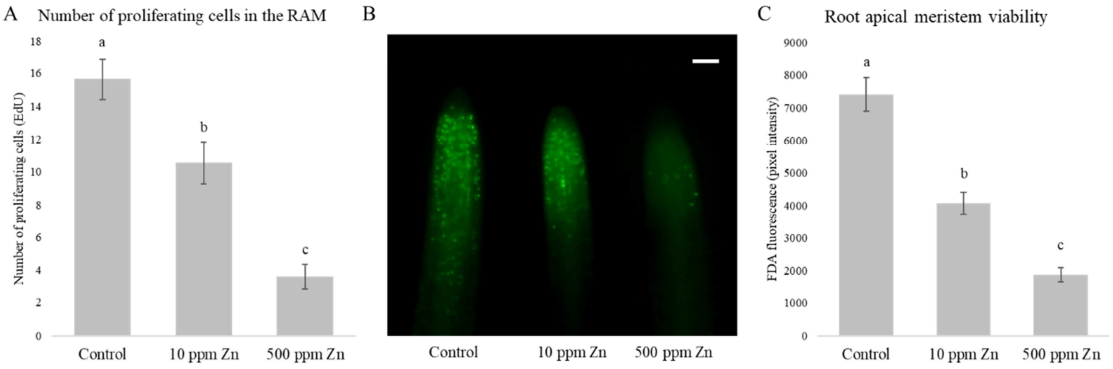

Fig. 7. (A) Number of cells with active DNA synthesis in the meristematic zone of the roots supplemented with 10 or 500 ppm Zn compared to the control (60 ppm total Zn). (B) Representative image of the root tips stained with EdU, showing the number and localisation of cells with active DNA synthesis in the root tips supplemented with 10 or 500 ppm Zn compared to the control (60 ppm total Zn) (bar=100µm). (C) Viability of the root apical meristem supplemented with 10 or 500 ppm Zn compared to the control (60 ppm total Zn). Different letters indicate significant differences according to Duncan-test (n=10-15, $P<0.05$).

4. Conclusions

The present study compared the effect of two different Zn supplementation on the rapeseed RSA and the underlying processes (summarised in Fig. 8). The two applied Zn concentrations triggered two completely different growth responses in *B. napus* root system. In the background of the 10 ppm Zn supplementation-induced positive growth response the pattern of tyrosine nitration rearranged significantly, and four new protein bands became nitrated. There were no severe disturbances in the nitro-oxidative signalling network; and due to the low Zn treatment and mild Zn uptake the composition of the cell walls changed only slightly in the root tips (pectin content increment). It has to be noted though, that despite the positive growth response, the viability of the root apical meristem cells decreased to some extent. On the other hand, 500 ppm Zn supplementation caused severe growth inhibition, what was co-occurred with increased tyrosine nitration. The nitro-oxidative balance was disturbed, both the fluorescence consistent with ROS and RNS formation increased significantly. Due to the high Zn concentration, Zn uptake was high in the root system and it caused severe alterations in the cell walls (both pectin and callose contents increased) and all these processes were coupled with a significant reduction in the viability of the root apical meristem.

Results suggest that Zn in different amounts triggers different root growth responses accompanied by distinct changes in the metabolism of ROS and RNS consequently resulting in alterations in pattern and intensity of protein tyrosine nitration. These suggest that nitrosative processes have an important role in zinc stress-induced root growth responses.

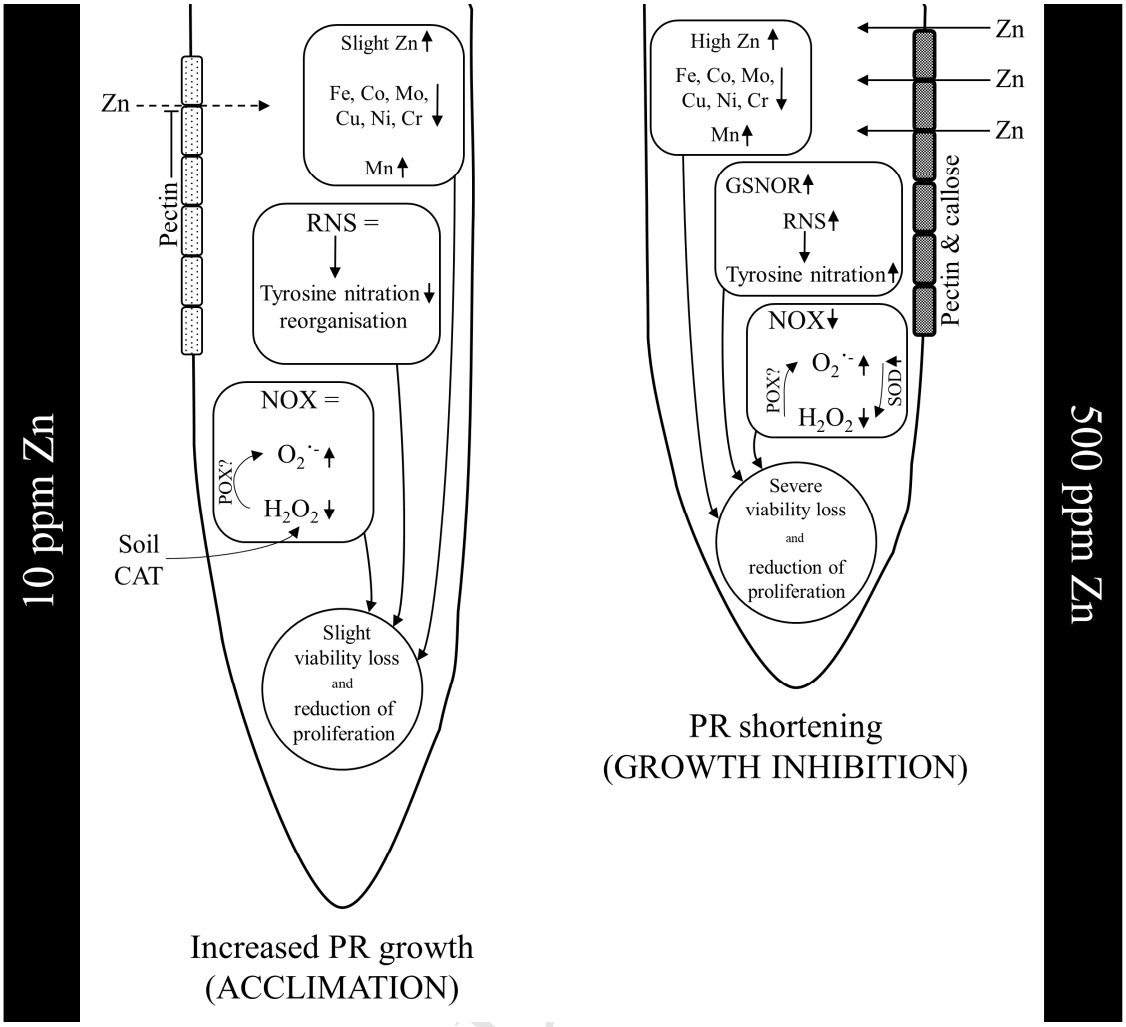

592

593 Fig. 8. Schematic model summarising the results presented in this study. 10 ppm Zn
594 supplementation caused a positive growth response with slight Zn uptake and tyrosine
595 nitration reorganisation in the background, while no oxidative or nitrosative stress was
596 detectable. 500 ppm Zn treatment inhibited root growth, and this stress response was
597 accompanied by high Zn uptake and indicated by increased cell wall modifications, tyrosine
598 nitration and fluorescence consistent with ROS/RNS formation. (An upward arrow indicates
599 increase while a downward arrow shows decrease; = means no significant change.)

5. Acknowledgements

This work was supported by the National Research, Development and Innovation Fund (Grant no. NKFI-1 PD 120962 and NKFI-6, K120383) and by the János Bolyai Research Scholarship of the Hungarian Academy of Sciences (Grant no. BO/00751/16/8). Zs. K. was supported by UNKP-18-4 New National Excellence Program of the Ministry of Human Capacities.

6. References

Andreini, C., Bertini, I., & Rosato, A. (2009). Metalloproteomes: a bioinformatic approach. Accounts of chemical research, 42(10), 1471-1479.

Apel, K., & Hirt, H. (2004). Reactive oxygen species: metabolism, oxidative stress, and signal transduction. Annu. Rev. Plant Biol., 55, 373-399.

Bacon, J. R., & Dinev, N. S. (2005). Isotopic characterisation of lead in contaminated soils from the vicinity of a non-ferrous metal smelter near Plovdiv, Bulgaria. Environmental Pollution, 134(2), 247-255.

Barroso, J. B., Corpas, F. J., Carreras, A., Rodríguez-Serrano, M., Esteban, F. J., Fernández-Ocana, A., ... & del Río, L. A. (2006). Localization of S-nitrosoglutathione and expression of S-nitrosoglutathione reductase in pea plants under cadmium stress. Journal of experimental botany, 57(8), 1785-1793.

Beauchamp, C., & Fridovich, I. (1971). Superoxide dismutase: improved assays and an assay applicable to acrylamide gels. Analytical biochemistry, 44(1), 276-287.

Begara-Morales, J. C., Chaki, M., Valderrama, R., Sánchez-Calvo, B., Mata-Pérez, C., Padilla, M. N., ... & Barroso, J. B. (2018). Nitric oxide buffering and conditional nitric oxide release in stress response. Journal of experimental botany, 69(14), 3425-3438.

Belyaeva, O. N., Haynes, R. J., & Birukova, O. A. (2005). Barley yield and soil microbial and enzyme activities as affected by contamination of two soils with lead, zinc or copper. Biology and Fertility of Soils, 41(2), 85-94.

Bi, X., Feng, X., Yang, Y., Qiu, G., Li, G., Li, F., ... & Jin, Z. (2006). Environmental contamination of heavy metals from zinc smelting areas in Hezhang County, western Guizhou, China. Environment international, 32(7), 883-890.

Bradford, M. M. (1976). A rapid and sensitive method for the quantitation of microgram quantities of protein utilizing the principle of protein-dye binding. Analytical biochemistry, 72(1-2), 248-254.

Broadley, M. R., White, P. J., Hammond, J. P., Zelko, I., & Lux, A. (2007). Zinc in plants. New phytologist, 173(4), 677-702.

Chen, X. Y., & Kim, J. Y. (2009). Callose synthesis in higher plants. Plant signaling & behavior, 4(6), 489-492.

Corpas, F. J., & Barroso, J. B. (2013). Nitro□oxidative stress vs oxidative or nitrosative stress in higher plants. New Phytologist, 199(3), 633-635.

Corpas, F. J., Luis, A., & Barroso, J. B. (2007). Need of biomarkers of nitrosative stress in plants. Trends in plant science, 12(10), 436-438.

Corpas, F. J., Leterrier, M., Valderrama, R., Airaki, M., Chaki, M., Palma, J. M., & Barroso, J. B. (2011). Nitric oxide imbalance provokes a nitrosative response in plants under abiotic stress. Plant Science, 181(5), 604-611.

Corpas, F. J., Palma, J. M., del Río, L. A., & Barroso, J. B. (2013). Protein tyrosine nitration in higher plants grown under natural and stress conditions. Frontiers in Plant Science, 4, 29.

Devienne-Barret, F., Richard-Molard, C., Chelle, M., Maury, O., & Ney, B. (2006). Ara-rhizotron: An effective culture system to study simultaneously root and shoot development of Arabidopsis. Plant and Soil, 280(1-2), 253-266.

Dhindsa, R. S., Plumb-Dhindsa, P., & Thorpe, T. A. (1981). Leaf senescence: correlated with increased levels of membrane permeability and lipid peroxidation, and decreased levels of superoxide dismutase and catalase. Journal of Experimental botany, 32(1), 93-101.

Durand, C., Vicré-Gibouin, M., Follet-Gueye, M. L., Duponchel, L., Moreau, M., Lerouge, P., & Driouich, A. (2009). The organization pattern of root border-like cells of Arabidopsis is dependent on cell wall homogalacturonan. Plant physiology, 150(3), 1411-1421.

Ebbs, S. D., & Kochian, L. V. (1997). Toxicity of zinc and copper to Brassica species: implications for phytoremediation. Journal of Environmental Quality, 26(3), 776-781.

Feigl, G., Lehotai, N., Molnár, Á., Ördög, A., Rodríguez-Ruiz, M., Palma, J. M., ... & Kolbert, Z. (2015). Zinc induces distinct changes in the metabolism of reactive oxygen and nitrogen species (ROS and RNS) in the roots of two Brassica species with different sensitivity to zinc stress. Annals of botany, 116(4), 613-625.

660 Feigl, G., Kolbert, Z., Lehotai, N., Molnár, Á., Ördög, A., Bordé, Á., ... & Erdei, L. (2016).
661 Different zinc sensitivity of Brassica organs is accompanied by distinct responses in protein
662 nitration level and pattern. Ecotoxicology and environmental safety, 125, 141-152.

663 Galetskiy, D., Lohscheider, J. N., Kononikhin, A. S., Popov, I. A., Nikolaev, E. N., &
664 Adamska, I. (2011). Phosphorylation and nitration levels of photosynthetic proteins are
665 conversely regulated by light stress. Plant molecular biology, 77(4-5), 461.

666 Gémes, K., Kim, Y. J., Park, K. Y., Moschou, P. N., Andronis, E., Valassaki, C., ... &
667 Roubelakis-Angelakis, K. A. (2016). An NADPH-oxidase/polyamine oxidase feedback loop
668 controls oxidative burst under salinity. Plant Physiology, 172(3), 1418-1431.

669 Gow, A. J., Farkouh, C. R., Munson, D. A., Posencheg, M. A., & Ischiropoulos, H. (2004).
670 Biological significance of nitric oxide-mediated protein modifications. American Journal of
671 Physiology-Lung Cellular and Molecular Physiology, 287(2), L262-L268.

672 Greenacre, S. A., & Ischiropoulos, H. (2001). Tyrosine nitration: localisation, quantification,
673 consequences for protein function and signal transduction. Free radical research, 34(6), 541-
674 581.

675 Hagmann, D. F., Goodey, N. M., Mathieu, C., Evans, J., Aronson, M. F., Gallagher, F., &
676 Krumins, J. A. (2015). Effect of metal contamination on microbial enzymatic activity in soil.
677 Soil Biology and Biochemistry, 91, 291-297.

678 Hall, J. L. (2002). Cellular mechanisms for heavy metal detoxification and tolerance. Journal
679 of experimental botany, 53(366), 1-11.

680 Jain, R., Srivastava, S., Solomon, S., Shrivastava, A. K., & Chandra, A. (2010). Impact of
681 excess zinc on growth parameters, cell division, nutrient accumulation, photosynthetic
682 pigments and oxidative stress of sugarcane (Saccharum spp.). Acta Physiologiae Plantarum,
683 32(5), 979-986.

684 Jain, A., Sinilal, B., Dhandapani, G., Meagher, R. B., & Sahi, S. V. (2013). Effects of
685 deficiency and excess of zinc on morphophysiological traits and spatiotemporal regulation of
686 zinc-responsive genes reveal incidence of cross talk between micro-and macronutrients.
687 Environmental science & technology, 47(10), 5327-5335.

688 Jones, D. L., Blancaflor, E. B., Kochian, L. V., & Gilroy, S. (2006). Spatial coordination of
689 aluminium uptake, production of reactive oxygen species, callose production and wall
690 rigidification in maize roots. Plant, cell & environment, 29(7), 1309-1318.

691 Jordan, M. O. (1992). Can rhizotrons be used for the study of corn (Zea mays L.) root
692 ramification? [needle board, root development, number of secondary roots]. Agronomie
693 (France) 12, 3–14.

694 Kalaivanan, D., Ganeshamurthy, A.N. (2016). Mechanisms of heavy metal toxicity in plants.
695 pp 21, in Rao, N. S., Shivashankara, K. S., & Laxman, R. H. (Eds.). (2016). Abiotic stress
696 physiology of horticultural crops. New Delhi: Springer. https://doi.org/10.1007/978-81-322-
697 2725-0

698 Kandeler, F., Kampichler, C., & Horak, O. (1996). Influence of heavy metals on the
699 functional diversity of soil microbial communities. Biology and fertility of soils, 23(3), 299-
700 306.

701 Kimura, M., Umemoto, Y., & Kawano, T. (2014). Hydrogen peroxide-independent generation
702 of superoxide by plant peroxidase: hypotheses and supportive data employing ferrous ion as a
703 model stimulus. Frontiers in plant science, 5, 285.

704 Kolbert, Z. (2016). Implication of nitric oxide (NO) in excess element-induced morphogenic
705 responses of the root system. Plant Physiology and Biochemistry, 101, 149-161.

706 Kolbert, Z. (2012). In vivo and in vitro studies on fluorophore-specificity. Acta Biologica
707 Szegediensis, 56(1), 37-41.

708 Kolbert, Z., Feigl, G., Bordé, Á., Molnár, Á., & Erdei, L. (2017). Protein tyrosine nitration in
709 plants: Present knowledge, computational prediction and future perspectives. Plant physiology
710 and biochemistry, 113, 56-63.

711 Kolbert, Z., Molnár, Á., Szőllősi, R., Feigl, G., Erdei, L., & Ördög, A. (2018). Nitro-oxidative
712 stress correlates with Se tolerance of Astragalus species. Plant and Cell Physiology, 59(9),
713 1827-1843.

714 Krumins, J. A., Goodey, N. M., & Gallagher, F. (2015). Plant–soil interactions in metal
715 contaminated soils. Soil Biology and Biochemistry, 80, 224-231.

716 Krzesłowska, M. (2011). The cell wall in plant cell response to trace metals: polysaccharide
717 remodeling and its role in defense strategy. Acta Physiologiae Plantarum, 33(1), 35-51.

718 Kurakov, A. V., Kupletskaya, M. B., Skrynnikova, E. V., & Somova, N. G. (2001). Search for
719 micromycetes producing extracellular catalase and study of conditions of catalase synthesis.
720 Applied Biochemistry and Microbiology, 37(1), 59-64.

721 Küpper, H., Lombi, E., Zhao, F. J., & McGrath, S. P. (2000). Cellular compartmentation of
722 cadmium and zinc in relation to other elements in the hyperaccumulator Arabidopsis halleri.
723 Planta, 212(1), 75-84.

724 Lehotai, N., Pető, A., Bajkán, S., Erdei, L., Tari, I., & Kolbert, Z. (2011). In vivo and in situ
725 visualization of early physiological events induced by heavy metals in pea root meristem.
726 Acta physiologiae plantarum, 33(6), 2199-2207.

727 Lehotai, N., Kolbert, Z., Pető, A., Feigl, G., Ördög, A., Kumar, D., ... & Erdei, L. (2012).
728 Selenite-induced hormonal and signalling mechanisms during root growth of Arabidopsis
729 thaliana L. Journal of experimental botany, 63(15), 5677-5687.

730 Lehotai, N., Lyubenova, L., Schröder, P., Feigl, G., Ördög, A., Szilágyi, K., ... & Kolbert, Z.
731 (2016). Nitro-oxidative stress contributes to selenite toxicity in pea (Pisum sativum L). Plant
732 and soil, 400(1-2), 107-122.

733 Lindermayr, C. (2018). Crosstalk between reactive oxygen species and nitric oxide in plants:
734 key role of S-nitrosoglutathione reductase. Free Radical Biology and Medicine, 122, 110-115.

735 Lingua, G., Franchin, C., Todeschini, V., Castiglione, S., Biondi, S., Burlando, B., ... & Berta,
736 G. (2008). Arbuscular mycorrhizal fungi differentially affect the response to high zinc
737 concentrations of two registered poplar clones. Environmental Pollution, 153(1), 137-147.

738 McCabe, P. F., & Leaver, C. J. (2000). Programmed cell death in cell cultures. In
739 Programmed Cell Death in Higher Plants (pp. 115-124). Springer, Dordrecht.
740 https://doi.org/10.1007/978-94-010-0934-8_9

741 Morina, F., Jovanovic, L., Mojovic, M., Vidovic, M., Pankovic, D., & Veljovic Jovanovic, S.
742 (2010). Zinc□induced oxidative stress in Verbascum thapsus is caused by an accumulation of
743 reactive oxygen species and quinhydrone in the cell wall. Physiologia plantarum, 140(3), 209-
744 224.

745 Mrozek Jr, E., & Funicelli, N. A. (1982). Effect of zinc and lead on germination of Spartina
746 alterniflora Loisel seeds at various salinities. Environmental and Experimental Botany, 22(1),
747 23-32.

748 Nakayama, H., Kawade, K., Tsukaya, H., & Kimura, S. (2015). Detection of the cell
749 proliferation zone in leaves by using EdU. Bio Protoc, 5, 18.

750 Nieboer, E., & Richardson, D. H. (1980). The replacement of the nondescript term 'heavy
751 metals' by a biologically and chemically significant classification of metal ions.
752 Environmental Pollution Series B, Chemical and Physical, 1(1), 3-26.

753 Noulas, C., Tziouvalekas, M., & Karyotis, T. (2018). Zinc in soils, water and food crops.
754 Journal of Trace Elements in Medicine and Biology, 49, 252-260.

755 Pagés, L. (1992). Root observation box for analysis of the root-system of young plants –
756 application to root development characterization of young oaks (Quercus robur). Canadian
757 Journal of Botany, 70(9), 1840-1847.

758 Pascual, I., Antolín, M. C., García, C., Polo, A., & Sánchez-Díaz, M. (2004). Plant
759 availability of heavy metals in a soil amended with a high dose of sewage sludge under
760 drought conditions. Biology and fertility of soils, 40(5), 291-299.

761 Peterson, C. A., & Rauser, W. E. (1979). Callose deposition and photoassimilate export in
762 Phaseolus vulgaris exposed to excess cobalt, nickel, and zinc. Plant Physiology, 63(6), 1170-
763 1174.

764 Pető, A., Lehotai, N., Feigl, G., Tugyi, N., Ördög, A., Gémes, K., ... & Kolbert, Z. (2013).
765 Nitric oxide contributes to copper tolerance by influencing ROS metabolism in Arabidopsis.
766 Plant cell reports, 32(12), 1913-1923.

767 Potters, G., Pasternak, T. P., Guisez, Y., Palme, K. J., & Jansen, M. A. (2007). Stress-induced
768 morphogenic responses: growing out of trouble?. Trends in plant science, 12(3), 98-105.

769 Potters, G., Pasternak, T. P., Guisez, Y., & Jansen, M. A. (2009). Different stresses, similar
770 morphogenic responses: integrating a plethora of pathways. Plant, cell & environment, 32(2),
771 158-169.

Radi, R. (2004). Nitric oxide, oxidants, and protein tyrosine nitration. Proceedings of the National Academy of Sciences, 101(12), 4003-4008.

Rezvani, M., & Zaefarian, F. (2011). Bioaccumulation and translocation factors of cadmium and lead in'Aeluropus littoralis'. Australian Journal of Agricultural Engineering, 2(4), 114.

Salic, A., & Mitchison, T. J. (2008). A chemical method for fast and sensitive detection of DNA synthesis in vivo. Proceedings of the National Academy of Sciences, 105(7), 2415-2420.

Sarkar, T. S., Biswas, P., Ghosh, S. K., & Ghosh, S. (2014). Nitric oxide production by necrotrophic pathogen Macrophomina phaseolina and the host plant in charcoal rot disease of jute: complexity of the interplay between necrotroph–host plant interactions. PLoS One, 9(9), e107348.

Sarret, G., Harada, E., Choi, Y. E., Isaure, M. P., Geoffroy, N., Fakra, S., ... & Manceau, A. (2006). Trichomes of tobacco excrete zinc as zinc-substituted calcium carbonate and other zinc-containing compounds. Plant Physiology, 141(3), 1021-1034.

Satbhai, S. B., Ristova, D., & Busch, W. (2015). Underground tuning: quantitative regulation of root growth. Journal of experimental botany, 66(4), 1099-1112.

Schindelin, J., Arganda-Carreras, I., Frise, E., Kaynig, V., Longair, M., Pietzsch, T., ... & Tinevez, J. Y. (2012). Fiji: an open-source platform for biological-image analysis. Nature methods, 9(7), 676.

Schützendübel, A., & Polle, A. (2002). Plant responses to abiotic stresses: heavy metal□ induced oxidative stress and protection by mycorrhization. Journal of experimental botany, 53(372), 1351-1365.

Seymour, J. L., & Lazarus, R. A. (1989). Native gel activity stain and preparative electrophoretic method for the detection and purification of pyridine nucleotide-linked dehydrogenases. Analytical biochemistry, 178(2), 243-247.

Sjölund, R. D. (1997). The phloem sieve element: a river runs through it. The Plant Cell, 9(7), 1137.

Stępniewska, Z., Wolińska, A., & Ziomek, J. (2009). Response of soil catalase activity to chromium contamination. Journal of Environmental Sciences, 21(8), 1142-1147.

Toal, T. W., Ron, M., Gibson, D., Kajala, K., Splitt, B., Johnson, L. S., ... & de Lucas, M. (2018). Regulation of Root Angle and Gravitropism. G3: Genes, Genomes, Genetics, g3-200540.

Tóth, G., Hermann, T., Da Silva, M. R., & Montanarella, L. (2016). Heavy metals in agricultural soils of the European Union with implications for food safety. Environment international, 88, 299-309.

Valderrama, R., Corpas, F. J., Carreras, A., Fernández-Ocaña, A., Chaki, M., Luque, F., ... & Barroso, J. B. (2007). Nitrosative stress in plants. Febs Letters, 581(3), 453-461.

Van Der Vliet, A., Eiserich, J. P., Shigenaga, M. K., & Cross, C. E. (1999). Reactive nitrogen species and tyrosine nitration in the respiratory tract: epiphenomena or a pathobiologic mechanism of disease?. American journal of respiratory and critical care medicine, 160(1), 1-9.

Wang, C., Zhang, S. H., Wang, P. F., Hou, J., Zhang, W. J., Li, W., & Lin, Z. P. (2009). The effect of excess Zn on mineral nutrition and antioxidative response in rapeseed seedlings. Chemosphere, 75(11), 1468-1476.

Wang, Y., Loake, G. J., & Chu, C. (2013). Cross-talk of nitric oxide and reactive oxygen species in plant programed cell death. Frontiers in Plant Science, 4, 314.

Wang, Y., Shi, J., Wang, H., Lin, Q., Chen, X., & Chen, Y. (2007). The influence of soil heavy metals pollution on soil microbial biomass, enzyme activity, and community composition near a copper smelter. Ecotoxicology and environmental safety, 67(1), 75-81.

Yoon, J., Cao, X., Zhou, Q., & Ma, L. Q. (2006). Accumulation of Pb, Cu, and Zn in native plants growing on a contaminated Florida site. Science of the total environment, 368(2-3), 456-464.

Yuan, P., Ding, G. D., Cai, H. M., Jin, K. M., Broadley, M. R., Xu, F. S., & Shi, L. (2016). A novel Brassica–rhizotron system to unravel the dynamic changes in root system architecture of oilseed rape under phosphorus deficiency. Annals of botany, 118(2), 173-184.

827 Zelko, I., Lux, A., Sterckeman, T., Martinka, M., Kollárová, K., & Lišková, D. (2012). An
828 easy method for cutting and fluorescent staining of thin roots. Annals of botany, 110(2), 475-
829 478.

830 Zhao, F. J., Lombi, E., & Breedon, T. M. S. P. (2000). Zinc hyperaccumulation and cellular
831 distribution in Arabidopsis halleri. Plant, Cell & Environment, 23(5), 507-514.

832 Zhao, F. J., Lombi, E., & McGrath, S. P. (2003). Assessing the potential for zinc and
833 cadmium phytoremediation with the hyperaccumulator Thlaspi caerulescens. Plant and soil,
834 249(1), 37-43.

Supplementary material

Supplementary video 1. Development of the root system architecture during the 10-day-long growing period. Rhizotrons were scanned daily and pictures were merged into a time-lapse to demonstrate the difference in the root growth dynamics of the control and 10 or 500 ppm Zn-supplemented *B. napus* plants.

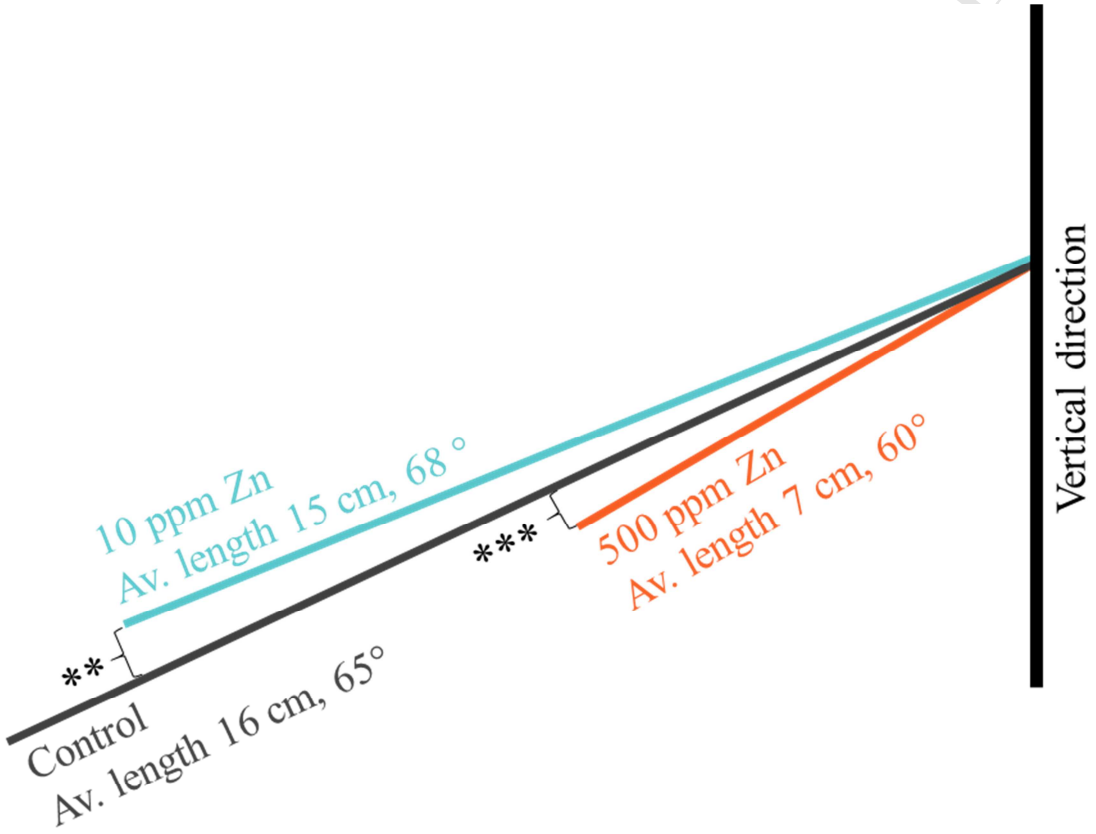

Supplementary figure 1. Schematic illustration of the occurred changes in the root system architecture of *B. napus* supplemented with different Zn concentrations: length of lateral roots and their angle with the vertical direction. Compared to the control lateral roots (average length 16 cm, angle 65°) 10 ppm Zn supplementation resulted shorter (15 cm) and more horizontal (68°) lateral root formation, while the addition of 500 ppm Zn inhibited lateral root length significantly (7 cm) growing in a more vertical direction (60°)

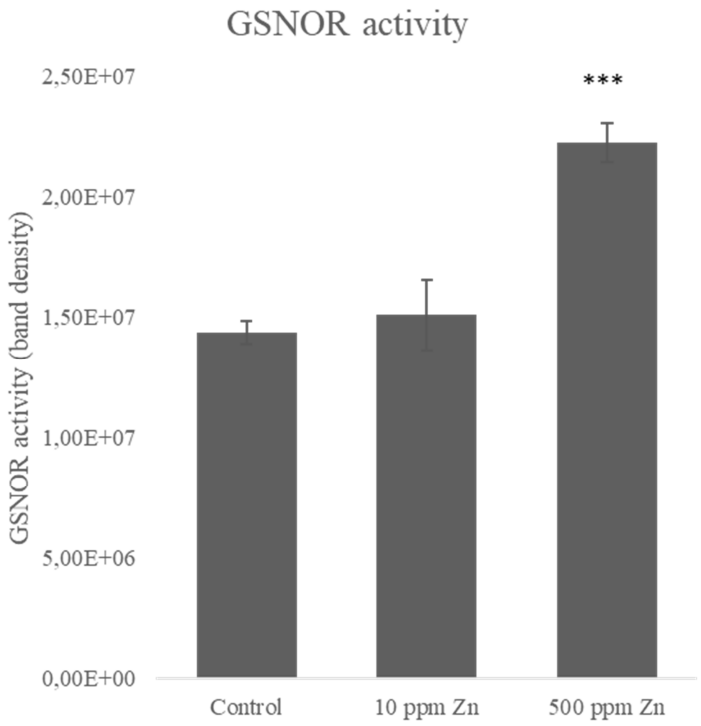

Supplementary figure 2. Changing of root-GSNOR activity of *B. napus* supplemented with 10 or 500 ppm Zn, compared to the control. Activity bands of GSNOR were quantified by Gelquant software provided by biochemlabsolutions.com (n=3).

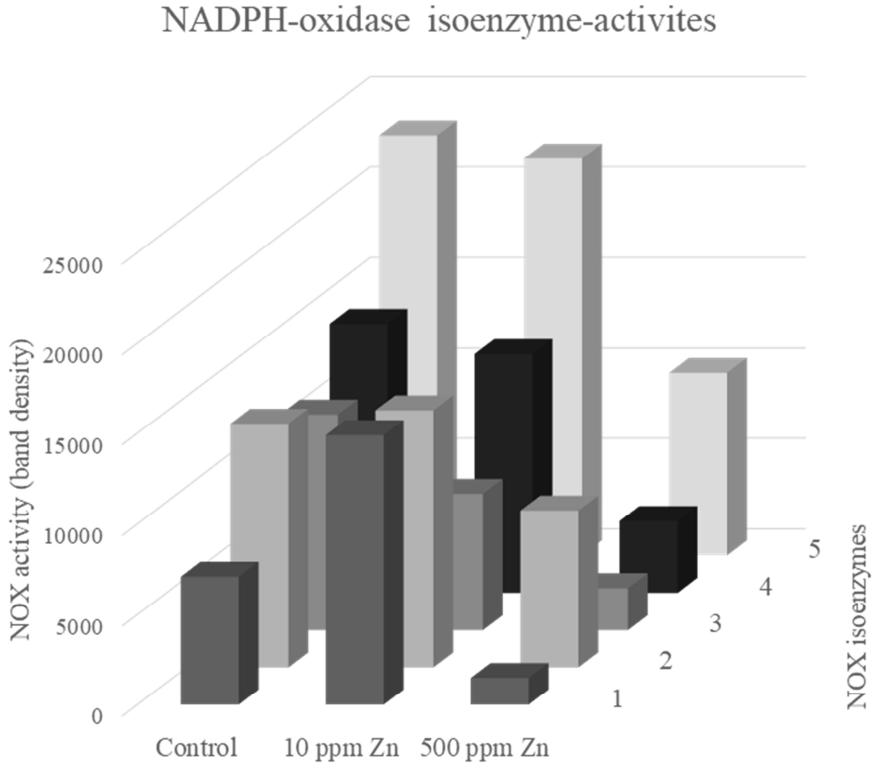

Supplementary figure 3. Changing the activities of the 5 putative isoenzymes of NADPH oxidase in *B. napus* roots supplemented with 10 or 500 ppm Zn, compared to the control. Activity bands of NOX isoenzymes were quantified by Gelquant software provided by biochemlabsolutions.com

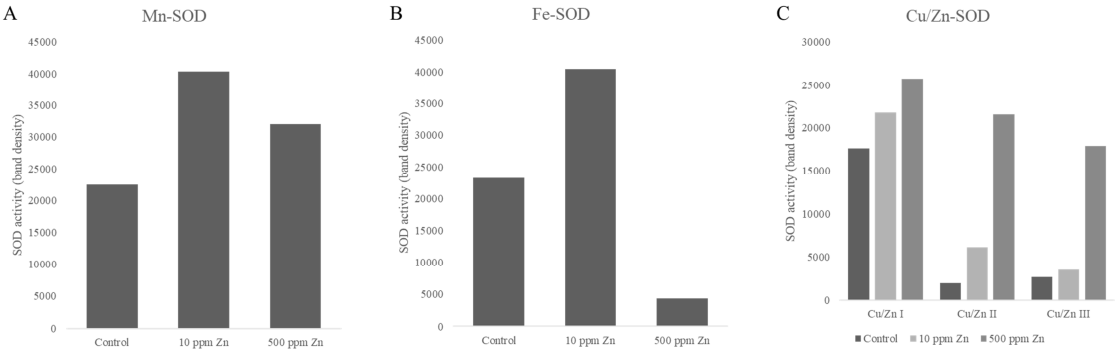

Supplementary figure 4. (A) Activity of Mn-SOD, (B) Fe-SOD and (C) Cu/Zn-SOD isoenzymes in *B. napus* roots treated with 10 or 500 ppm Zn, compared to the control. Activity bands of SOD isoenzymes were quantified by Gelquant software provided by biochemlabsolutions.com

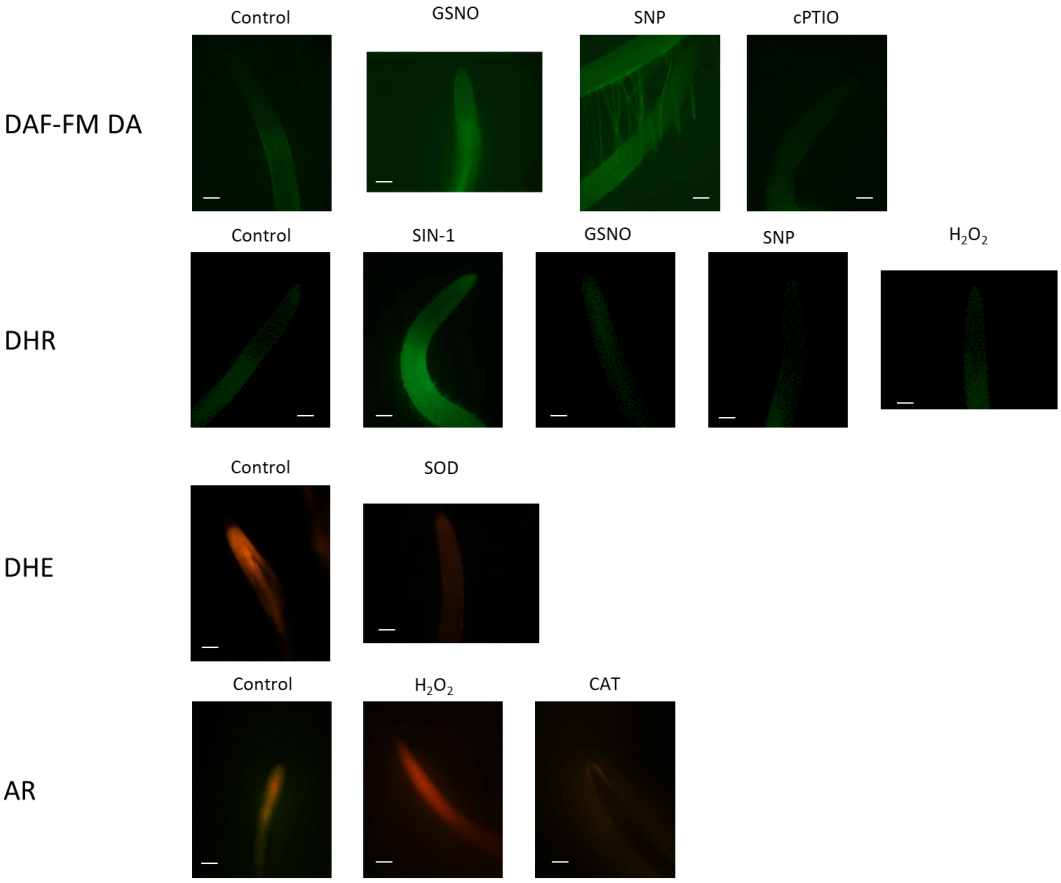

867

868 Supplementary figure 5. Representative images showing controls for DAF-FM DA, DHR,
869 DHE and Amplex Red (AR) fluorescent probes in *B. napus* roots. Root tips were incubated
870 for 1 hour in the presence of distilled water (controls) or 400 µM S-nitrosoglutathione
871 (GSNO, nitric oxide donor), 200 µM sodium nitroprusside (SNP, nitric oxide donor), 400 µM
872 2-4-carboxyphenyl-4,4,5,5-tetramethylimidazoline-1-oxyl-3-oxide (cPTIO, nitric oxide
873 scavenger), 1 mM 3-morpholinosydnonimine (SIN-1, peroxynitrite donor), 10 mM hydrogen
874 peroxide (H2O2), 200 U superoxid dismutase (SOD) or 200 U catalase (CAT). Then roots
875 were incubated in fluorophore solutions as described in Materials and methods. Bars=100µm.

876